

UNITARY CYCLIC ESPRIT ALGORITHM IN THE PRESENCE OF COHERENT SIGNALS

Zhi-Gang Liu and Jin-Kuan Wang
 Institute of Information and Engineering
 Northeastern University
 Shenyang, China
 email: zliu@neuq.edu.cn

1. Introduction

Popular DOA methods, such as MUSIC [1] and ESPRIT [2], are known to yield high resolution but suffer from three drawbacks. Firstly the total number of signals impinging on the array, including both signals of interest (SOIs) and interference, is less than the number of sensors or the characteristics of interfering signals are known so that their effects can be subtracted; secondly it is impossible to resolve two signals spaced more closely than the resolution threshold of the array when only one signal is a SOI; thirdly the noise characteristics of the sensors and the environment are known or they are accurately modelled as independent and identically distributed gaussian random processes. Therefore signal selective Cyclic MUSIC [3]-[4] and Cyclic ESPRIT [5] presented effectively overcome these drawbacks by exploiting the differing spectral correlation characteristics of the different signals. These cyclic algorithms perform poorly when coherent or highly correlated signals are present. Thus a signal selective Unitary Cyclic ESPRIT algorithm is proposed to circumvent the drawback, which has a better performance in the presence of multipath propagation in this paper. This algorithm not only reduces the computational complexity by real-valued eigendecomposition, but also allows to select desired signals and to ignore interferences by exploiting the cyclostationarity property of the SOIs.

2. Cyclic ESPRIT algorithm

Consider a Uniform Linear Array (ULA) composed of m omnidirectional sensors. Suppose d narrowband farfield sources with center frequency w_0 impinging from the directions $\theta_1, \dots, \theta_d$. Assume that there are N snapshots $\mathbf{x}(1), \mathbf{x}(2), \dots, \mathbf{x}(N)$ available, the observation vector can be modelled as

$$\mathbf{x}(k) = \mathbf{A}\mathbf{s}(k) + \mathbf{i}(k) + \mathbf{n}(k) \quad (1)$$

where $\mathbf{A} = [\mathbf{a}(\theta_1), \dots, \mathbf{a}(\theta_d)]$ is the $m \times d$ matrix of the signal direction vectors, and $\mathbf{a}(\theta_i)$ is the $m \times 1$ steering vector. And $\mathbf{s}(k) = [s_1(k), \dots, s_d(k)]^T$ is the vector of cyclostationary signals with cycle frequency α . $\mathbf{i}(k)$ is the vector of interfering sources with cyclostationary property, and $\mathbf{n}(k)$ is the vector of sensor noise. Hence for some cyclic frequency α and some lag parameter τ , the cyclic autocorrelation matrix of the observation vector is defined by

$$\mathbf{R}_{\mathbf{xx}}^\alpha(\tau) = \langle \mathbf{x}(k)\mathbf{x}^H(k+\tau)e^{-j2\pi\alpha k} \rangle = \mathbf{A}\mathbf{R}_{\mathbf{ss}}^\alpha(\tau)\mathbf{A}^H \quad (2)$$

where

$$\mathbf{R}_{\mathbf{ss}}^\alpha(\tau) = \langle \mathbf{s}(k)\mathbf{s}^H(k+\tau)e^{-j2\pi\alpha k} \rangle \quad (3)$$

is the $d \times d$ cyclic autocorrelation matrix of the cyclostationary signal vector. $\langle \cdot \rangle$ denotes the finite time average operator, and superscript H denotes complex conjugate transpose of a vector or matrix. Depending on type of modulation used, the cycle frequency α is usually equal to the twice of the carrier frequency, multiple of the baud rate, spreading codes repetition rate, chip rate or combinations of these. Compared with the covariance matrix exploited by ESPRIT algorithm, the cyclic autocorrelation matrix exploited by the Cyclic ESPRIT method is generally not Hermitian. Then, instead of using the eigenvalue decomposition (EVD), Cyclic ESPRIT algorithm uses the singular value decomposition (SVD) as follows

$$\mathbf{R}_{\mathbf{xx}}^\alpha(\tau) = [\mathbf{U}_s \ \mathbf{U}_n] \begin{bmatrix} \sum_s & \mathbf{0} \\ \mathbf{0} & \sum_n \end{bmatrix} [\mathbf{V}_s \ \mathbf{V}_n]^H \quad (4)$$

Obviously, the structure of steering vector matrix \mathbf{A} implies that it can be decomposed into $\mathbf{A}_1, \mathbf{A}_2 \in C^{m-1 \times d}$ such that the relationship [6] between them can be written as

$$\mathbf{A}_2 = \mathbf{A}_1\Phi \quad (5)$$

where $\Phi = \text{diag}\{e^{-jw_0\tau_1}, e^{-jw_0\tau_2}, \dots, e^{-jw_0\tau_d}\}$ is a rotation operator. If the cyclic autocorrelation matrix of the cyclostationary signal vector $\mathbf{R}_{\mathbf{ss}}^\alpha(\tau)$ is nonsingular, \mathbf{A} and \mathbf{U}_s share a common column space as follows

$$R(\mathbf{A}) = R(\mathbf{U}_s) \quad (6)$$

Thus there must exist a unique nonsingular \mathbf{T} such that

$$\mathbf{A}\mathbf{T} = \mathbf{U}_s \quad (7)$$

Furthermore, in conjunction with \mathbf{A}_1 and \mathbf{A}_2 , \mathbf{U}_1 and \mathbf{U}_2 are obtained by the relation

$$\mathbf{U}_2 = \mathbf{U}_1\Psi \quad (8)$$

where Φ and Ψ have the same eigenvalues. Finally, DOAs of SOIs by these eigenvalues are estimated.

3. Unitary Cyclic ESPRIT algorithm

Let a ULA with L identical sensors $\{1, \dots, L\}$ be divided into overlapping subarrays of size m , with sensors $\{1, \dots, m\}$ forming the first subarray, sensors $\{2, \dots, m+1\}$ forming the second subarray, etc. Thus the vector of received signals at the p th subarray can be written as follows

$$\mathbf{x}_p(k) = \mathbf{A}\Phi^{(p-1)}\mathbf{s}(k) + \mathbf{i}_p(k) + \mathbf{n}_p(k) \quad (9)$$

where Φ denotes the p th power of $d \times d$ diagonal matrix. Then the forward covariance matrix of the p th subarray is defined by

$$\mathbf{R}_p^\alpha(\tau) = \mathbf{A}\Phi^{(p-1)}\mathbf{S}_p^\alpha(\tau)[\Phi^{(p-1)}]^H\mathbf{A}^H \quad (10)$$

where $\mathbf{S}_p^\alpha(\tau)$ is therefore given by

$$\mathbf{S}_p^\alpha(\tau) = \mathbf{R}_{ss}^\alpha(\tau)[\Phi^{(p-1)}]^H\mathbf{A}^H\mathbf{A}\Phi^{(p-1)}[\mathbf{R}_{ss}^\alpha(\tau)]^H \quad (11)$$

and the backward covariance matrix of the p th subarray is defined as follows

$$\begin{aligned} \bar{\mathbf{R}}_p^\alpha(\tau) &= \mathbf{J}\mathbf{A}^*[\Phi^{(p-1)}]^*[\mathbf{S}_p^\alpha(\tau)]^*[\Phi^{(p-1)}]^{*H}\mathbf{A}^{*H}\mathbf{J} \\ &= \mathbf{A}\Phi^{(2-m-p)}[\mathbf{S}_p^\alpha(\tau)]^*[\Phi^{(2-m-p)}]^H\mathbf{A}^H \end{aligned} \quad (12)$$

where $\mathbf{J} \in C^{d \times d}$ is the exchange matrix with ones on its antidiagonal and zeros elsewhere and superscript $*$ denotes complex conjugation. So the forward backward smoothed covariance matrix [7]-[8] is introduced by

$$\tilde{\mathbf{R}}_{FB}^\alpha(\tau) = \frac{1}{2P} \sum_{p=1}^P (\mathbf{R}_p^\alpha(\tau) + \bar{\mathbf{R}}_p^\alpha(\tau)) \quad (13)$$

or more compactly as

$$\tilde{\mathbf{R}}_{FB}^\alpha(\tau) = \mathbf{A}\mathbf{S}_{FB}^\alpha(\tau)\mathbf{A}^H \quad (14)$$

where $\mathbf{S}_{FB}^\alpha(\tau)$, the modified cyclic autocorrelation matrix of the cyclostationary signals, is given by

$$\mathbf{S}_{FB}^\alpha(\tau) = \frac{1}{2P} \sum_{p=1}^P (\Phi^{(p-1)}\mathbf{S}_p^\alpha(\tau)[\Phi^{(p-1)}]^H + \Phi^{(2-m-p)}[\mathbf{S}_p^\alpha(\tau)]^*[\Phi^{(2-m-p)}]^H) \quad (15)$$

A complex matrix \mathbf{G} is called centro-Hermitian [9]-[10] if $\mathbf{G} = \mathbf{J}\mathbf{G}^*\mathbf{J}$. Thus, the modified cyclic autocorrelation matrix $\tilde{\mathbf{R}}_{FB}^\alpha(\tau)$ is centro-Hermitian.

By exploiting the centro-Hermitian property of $\tilde{\mathbf{R}}_{FB}^\alpha(\tau)$, we introduce the real-valued covariance matrix as

$$\mathbf{C} = \mathbf{Q}^H\tilde{\mathbf{R}}_{FB}^\alpha(\tau)\mathbf{Q} \quad (16)$$

where \mathbf{Q} is any unitary column conjugate symmetric matrix, for example

$$\mathbf{Q} = \frac{1}{\sqrt{2}} \begin{bmatrix} \mathbf{I} & j\mathbf{I} \\ \mathbf{J} & -j\mathbf{J} \end{bmatrix}, \mathbf{Q} = \frac{1}{\sqrt{2}} \begin{bmatrix} \mathbf{I} & \mathbf{0} & j\mathbf{I} \\ \mathbf{0}^T & \sqrt{2} & \mathbf{0}^T \\ \mathbf{J} & \mathbf{0} & -j\mathbf{J} \end{bmatrix}$$

can be chosen for arrays with an even and odd number of sensors, respectively, where \mathbf{I} is the identity matrix and $\mathbf{0}$ is the vector $[0, 0, \dots, 0]^T$. Compared with the modified cyclic autocorrelation matrix (14), the real-valued covariance matrix is obtained as

$$\mathbf{C} = \tilde{\mathbf{A}}\mathbf{S}_{FB}^\alpha(\tau)\tilde{\mathbf{A}}^H \quad (17)$$

where $\tilde{\mathbf{A}} = \mathbf{Q}^H\mathbf{A}$ denotes the relationship between the former and new manifolds.

Contrary to the cyclic covariance matrix $\mathbf{R}_{xx}^\alpha(\tau)$ exploited by Cyclic ESPRIT algorithm, the forward backward smoothed covariance matrix $\tilde{\mathbf{R}}_{FB}^\alpha(\tau)$ presented is Hermitian. Let the eigendecompositions of the matrices (13) and (14) be defined as

$$\tilde{\mathbf{R}}_{FB}^\alpha(\tau) = \mathbf{U}\mathbf{\Lambda}\mathbf{U}^H = \mathbf{U}_s\mathbf{\Lambda}_s\mathbf{U}_s^H + \mathbf{U}_n\mathbf{\Lambda}_n\mathbf{U}_n^H \quad (18)$$

$$\mathbf{C} = \mathbf{E}\mathbf{\Gamma}\mathbf{E}^H = \mathbf{E}_s\mathbf{\Gamma}_s\mathbf{E}_s^H + \mathbf{E}_n\mathbf{\Gamma}_n\mathbf{E}_n^H \quad (19)$$

where

$$\begin{aligned} \mathbf{U}_s &= [u_1, \dots, u_d], \mathbf{U}_n = [u_{d+1}, \dots, u_m] \\ \mathbf{\Lambda}_s &= \text{diag}\{\lambda_1, \dots, \lambda_d\}, \mathbf{\Lambda}_n = \text{diag}\{\lambda_{d+1}, \dots, \lambda_m\} \\ \mathbf{E}_s &= [\varepsilon_1, \dots, \varepsilon_d], \mathbf{E}_n = [\varepsilon_{d+1}, \dots, \varepsilon_m] \\ \mathbf{\Gamma}_s &= \text{diag}\{\gamma_1, \dots, \gamma_d\}, \mathbf{\Gamma}_n = \text{diag}\{\gamma_{d+1}, \dots, \gamma_m\} \end{aligned}$$

and the subscripts s and n stand for signal- and null-space, respectively. The characteristic equation for the matrix (13) is written as

$$\tilde{\mathbf{R}}_{FB}^\alpha(\tau)u = \lambda u \quad (20)$$

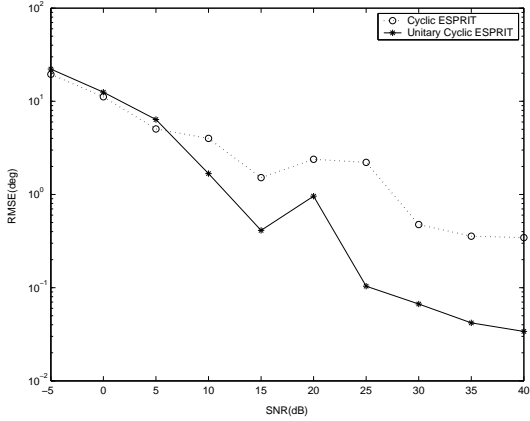


Fig. 1. Spatial spectra for environment containing two uncorrelated SOIs with -15° and -25° DOA and one interferer with 15° DOA.

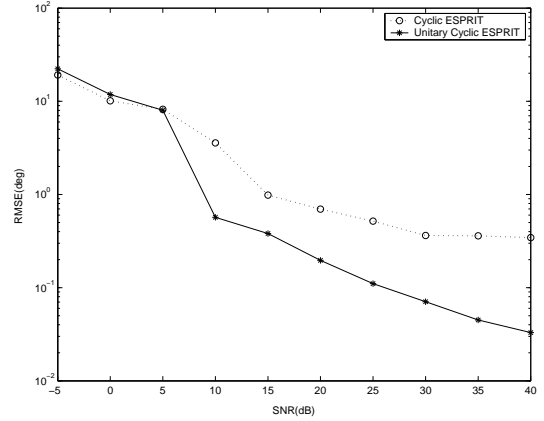


Fig. 2. Spatial spectra for environment containing two coherent SOIs with -15° and -25° DOA and one interferer with 15° DOA.

which can be further rewritten as

$$\begin{aligned} \mathbf{Q}^H \tilde{\mathbf{R}}_{FB}^\alpha(\tau) u &= \mathbf{Q}^H \tilde{\mathbf{R}}_{FB}^\alpha(\tau) \mathbf{Q} \mathbf{Q}^H u \\ &= \mathbf{C} \mathbf{Q}^H u \\ &= \lambda u \end{aligned} \quad (21)$$

Equation (21) can be identified as the characteristic one for the real-valued covariance matrix (16). Hence, the eigenvectors and eigenvalues of the matrices (14) and (16) are related as

$$\mathbf{E} = \mathbf{Q}^H \mathbf{U} \quad (22)$$

Thus, using equations (6) and (22), the important relationship between \mathbf{A} and $\tilde{\mathbf{E}}_s$ is obtained as

$$R(\mathbf{A}) = R(\tilde{\mathbf{E}}_s) \quad (23)$$

where

$$\tilde{\mathbf{E}}_s = \mathbf{Q} \mathbf{E}_s \quad (24)$$

In addition, in conjunction with \mathbf{U}_1 and \mathbf{U}_2 , $\tilde{\mathbf{E}}_1$ and $\tilde{\mathbf{E}}_2$ are extracted from the matrix $\tilde{\mathbf{E}}_s$.

Summary of Unitary Cyclic ESPRIT algorithm:

- Step 1: Choose the cycle frequency of desired signals α and the optimal τ ;
- Step 2: Estimate the forward backward smoothed co-variance matrix $\tilde{\mathbf{R}}_{FB}^\alpha(\tau)$ from the received data of ULA;
- Step 3: Form the real-valued matrix \mathbf{C} with the use of (16);
- Step 4: Find the signal subspace \mathbf{E}_s of the real-valued matrix \mathbf{c} , and detect the number d of SOIs based on AIC and MDL principle;
- Step 5: Based on equations (22) and (24), form $\tilde{\mathbf{E}}_1$ and $\tilde{\mathbf{E}}_2$;
- Step 6: Calculate the eigenvalues $\phi_k (k = 1, \dots, d)$ of matrix pencil $\{\tilde{\mathbf{E}}_1, \tilde{\mathbf{E}}_2\}$;
- Step 7: Estimate DOAs of SOIs by these eigenvalues.

4. Simulation Results

In this section, we present some simulation results to show the behavior of Unitary Cyclic ESPRIT algorithm and to compare it with the Cyclic ESPRIT algorithm. Assume a ULA with eight omnidirectional sensors spaced by a half wavelength of the coming signals. Incoming cyclostationary signals with central frequency 0.1 are generated with noise at cycle frequency 0.2.

In the first simulation, the performance of Unitary Cyclic ESPRIT algorithm is affected by SNR. Two uncorrelated SOIs arrive from -15° and -25° . The results for Cyclic ESPRIT and Unitary Cyclic ESPRIT versus the SNR are plotted in Fig. 1. In the second simulation, the performance of Unitary Cyclic ESPRIT algorithm is affected by SNR in the presence of interfering. Two uncorrelated SOIs arrive from -15° and -25° , and one interferer arrives from 15° . The results for them are shown in Fig. 2. In the third simulation, the performance of Unitary Cyclic ESPRIT algorithm is affected by SNR for coherent signals. Two coherent signals arrive from -15° and -25° . The results for them are shown in Fig. 3. In the fourth simulation, the performance of Unitary Cyclic ESPRIT algorithm is affected by SNR in the presence of interfering for coherent signals. Two coherent signals arrive from -15° and -25° , and one interferer arrives from 15° . The results for them are shown in Fig. 4.

Figs. 1-2 show how the SNR affects the DOA estimation for uncorrelated signals. And Figs. 3-4 show how the SNR affects the DOA estimation for coherent signals. The performance of the method is quantified by the root-mean-square-error (RMSE) of 200 independent DOA estimates. Unitary Cyclic ESPRIT algorithm and Cyclic ESPRIT algorithm can separate uncorrelated signals, but only Unitary Cyclic ESPRIT algorithm can separate coherent signals. As expected, the presence of the interfering has little effect on the SOIs. Therefore Unitary Cyclic ESPRIT algorithm performs better than the Cyclic ESPRIT algorithm, both for correlated and uncorrelated source scenarios.

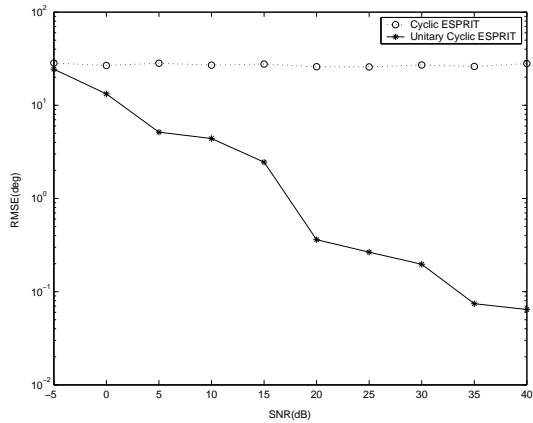


Fig. 3. Spatial spectra for environment containing two uncorrelated SOIs with -15° and -25° DOA and one interferer with 15° DOA.

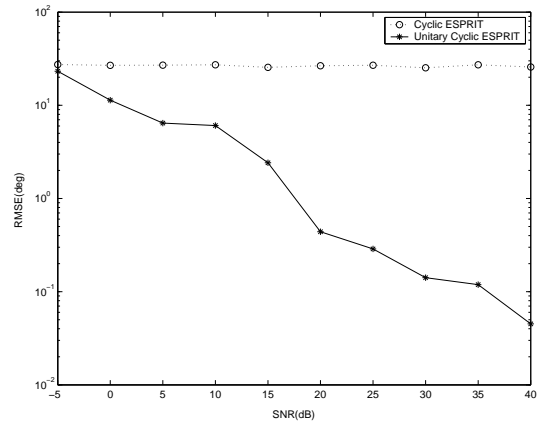


Fig. 4. Spatial spectra for environment containing two coherent SOIs with -15° and -25° DOA and one interferer with 15° DOA.

5. Conclusion

Unitary Cyclic ESPRIT algorithm is proposed by constructing a new forward backward smoothed covariance matrix in this paper. Simulation results suggest that the proposed approach has a better signal selectivity and a better resolution power than Cyclic ESPRIT algorithm, by exploiting the property of the cyclostationarity of incoming signals, both for correlated and uncorrelated source scenarios. At the same time this approach has low computational complexity because of real-valued computation.

References

- [1] R.O. Schmidt, "Multiple emitter location and signal parameter estimation," IEEE Trans AP, Vol. AP-34, pp.276-280, Mar. 1986.
- [2] R. Roy, T. Kailath, "ESPRIT-estimation of signal parameters via rotational invariance techniques," IEEE Trans. ASSP, vol. 37, pp. 984-995, Jul. 1989.
- [3] S. V. Schell, R. A. Calabreta, W. A. Gardner, and B. G. Agee, "Cyclic MUSIC algorithms for signal-selective DOA estimation," in Proc. IEEE ICASSP, Glasgow, U.K., pp.2278-2281, May 1989.
- [4] P. Charge, Y. Wang, and J. Sillard, "An extended Cyclic MUSIC algorithm," IEEE Trans. SP, Vol. 51, pp.1695-1701, Jul. 2003.
- [5] L. Jin, M. L. Yao, and Q. Y. Yin, "New model for the DOA estimation of the coherent signals," Proceeding of IEEE international symposium on Circuits and Systems, pp.329-332, Monterey, 1998.
- [6] J. K. Wang, Z. G. Liu, Y. B. Xue, et al, "An modified ESPRIT using spatial smoothing Technique," Control and Decision, Vol.19, pp.96-98, Jan. 2004.
- [7] T. J. Shan, M. Wax, and T. Kailath, "On spatial smoothing for direction-of-arrival estimation of coherent signals," IEEE Trans. ASSP, vol. ASSP-33, pp. 806-811, Aug. 1985.
- [8] R. T. Williams, S. Prasad, A. K. Mahalanabis, and L. H. Sibul, "An improved spatial smoothing technique for bearing estimation in a multipath environment," IEEE Trans. ASSP, vol. 36, pp.425-432, Apr. 1988.
- [9] M. Haardt, and J. A. Nossek, "Unitary ESPRIT: how to obtain increased estimation accuracy with a reduced computational burden," IEEE Trans SP, vol. 43, pp. 1232-1242, May 1995.
- [10] M. Pesavento, A. B. Gershman, and M. Haardt, "Unitary root-MUSIC with a real-valued eigendecomposition: a theoretical and experimental performance study," IEEE Trans. SP, vol. 48, pp.1306-1314, May 2000.



Zhi-Gang Liu received the B.Eng. degree from Northeastern University at Qinhuangdao and the M.Eng. degree from Northeastern University, Shenyang, in 2001 and 2004, respectively. In 2002, he joined Key Program of Science and Technology from the Ministry of Education of China, under Grant no. 02085. His research interests include adaptive signal processing and parameter identification.



Jin-Kuan Wang received the M. Eng. Degree from Northeastern University, Shenyang, China, in 1985 and the Ph.D. degree from the University of Electro-Communications, Japan, in 1993. As a special member, he joined the Institute of Space and Astronautical Science, Japan, in 1990. And he worked as an engineer in Research Department of COSEL company, Japan, in 1994. He is currently a professor in the Institute of Information and Engineering at Northeastern University, China, since 1998. His main interests are in the area of Intelligent Control and Adaptive Array.